BULGARIAN ACADEMY OF SCIENCES
JOURNAL OF THEORETICAL
AND APPLIED MECHANICS
Sofia, 1991, Year XXII, No 3

J. Frączak

Numerical Simulation of Separated Flow Past a Circular Cylinder by a Discrete-Vortex Method

1. Introduction

Based on the discrete vortex method introduced by Rosenhead [1] for approximate representation of the continuously distributed vorticity in an inviscid incompressible fluid by a discrete line vortices, a number of numerical studies have been carried out concerning the time development of the separated flow around a circular cylinder. The weakness of these methods lies in the mechanism of introducing vorticity into the flow. The detachment site of the shear layer from the circular cylinder surface is not fixed and this is the reason why various assumptions about the separation points are made. A review of the suitable numerical techniques applied to match real fluid effects is given in [2, 3].

For sufficiently high Reynolds numbers (laminar regime 10^4—10^5) the flow may be divided into two subregions: a viscous inner flow near the cylinder, described as boundary layer and an essentially inviscid external flow outside this area. The external flow consists of an irrotational flow outside the boundary layer and the wake.

The paper deals with numerical simulation of a two-dimensional incompressible time dependent flow past a circular cylinder in an impulsively started uniform stream of an inviscid fluid. The approach is based on the potential flow model and its extension covering viscosity effects indirectly by the artificially fixed mean position of the flow separation depending on the Reynolds number. Applying the well-known discrete-vortex method a relatively simple model has been formulated for unsteady separated flow past a circular cylinder with vortex shedding. For the sake of simplicity all results are presented in terms of nondimensional quantities. The dependent and independent variables are normalized as follows:

$$W'(z)=W(z)/U_\infty R^2,\quad z'=z/R,\quad \Gamma'=\Gamma/U_\infty R,\quad t=U_\infty t/R,\quad u'=u/U_\infty,$$
$$v'=v/U_\infty,\quad \theta'=\theta,\quad C_D=D/\rho RU_\infty^2,\quad C_L=L/\rho RU_\infty^2,\quad S=2fR/U_\infty,\quad Re=2RU_\infty/\nu,$$

where dimensional quantities are represented by W — complex velocity potential, U_∞ — uniform flow velocity, R — cylinder radius, z — complex variable, Γ — circulation, t — time, u, v — Cartesian velocity components, D — drag, L — lift, ρ — density of fluid, f — vortex shedding frequency, ν — kinematic viscosity of fluid, respectively, and nondimensional quantities are respectively represented by θ — polar angle, C_D — drag coefficient, C_L — lift coefficient, S — Strouhal number, Re — Reynolds number. Further on, primes are dropped from the symbols dimensionless variables.

2. Mathematical representation of the flow field

The complex velocity potential $W(z)$ in the physical plane z generated by the uniform flow in the positive x — direction, a dublet at the origin of the coordinate

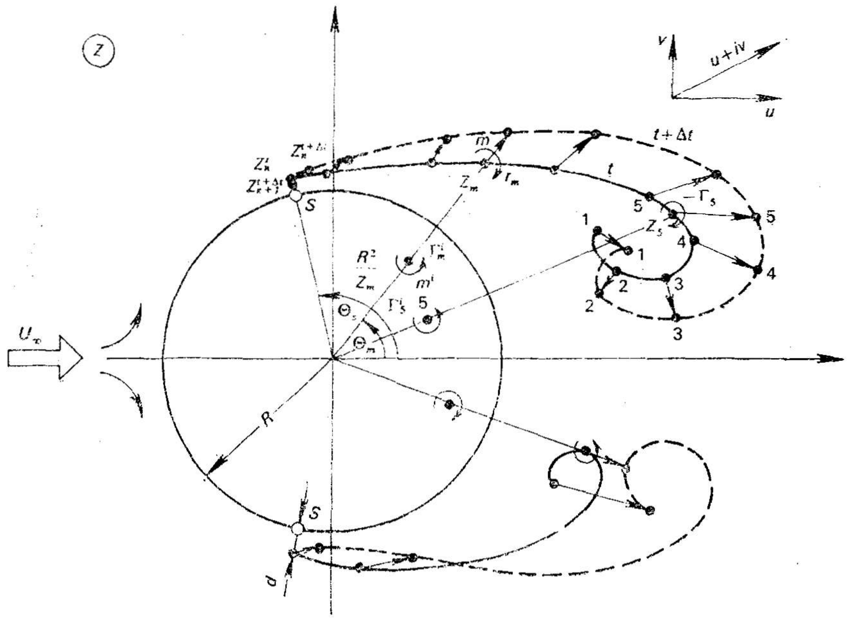

Fig. 1. Simplified model of the flow

system to simulate the cylinder, N real vortices in the wake, and N image vortices in the cylinder (Fig. 1) can be written down as

$$W(z)=z+\frac{1}{z}-\frac{i}{2\pi}\sum_{n=1}^{N}\Gamma_n\left[\ln(z-z_n)-\ln\left(z-\frac{1}{\bar{z}_n}\right)\right], \tag{1}$$

where $z=x+iy$, $i=\sqrt{-1}$

whilst Γ_n and z_n represent the strength (positive when rotating counterclockwise) and location of the nth vortex, respectively, the overbar indicates a complex conjugate. Each vortex has an image of opposite sign at its inverse point to ensure that the normal component velocity on the cylinder surface vanishes everywhere and that the total vorticity in the flow is always zero. There are no images at the centre of the cylinder because the vortices having beed shed from it, leave circulation opposite to their own on the cylinder [4, 5]. Hence, the total vorticity is equal to zero. The complex velocity at any point $z=x+iy$ is given by

$$\frac{dW}{dz}=u-iv=1-\frac{1}{z^2}-\frac{i}{2\pi}\sum_{n=1}^{N}\Gamma_n\left[\frac{1}{z-z_n}-\frac{1}{z-\frac{1}{\bar{z}_n}}\right], \tag{2}$$

where u and v respectively are the x and y velocity components.

3. Generation of vortices and the separation condition

Shortly after an impulsive start the boundary layer approaches the quasi-steady state. It is known [6, 7] that at subcritical Reynolds numbers the separation points do not fluctuate perceptibly. Thus, the mean position of flow separation point (depending on the Reynolds number) can be determined from experimental data [8]. In the numerical model the generation of vorticity in the boundary layer at the upstream section of the cylinder surface is simulated by introducing new vortices at a constant frequency, e. g. at each time step of computation two new point vortices with opposite sence of rotation are introduced into the flow at the boundary layer separation points $\theta=\theta_s$ [4, 9] obtained from experimental data [10, 11].

The position and strength of each new introduced vortex are determined by applying the no-slip condition at the separation [12]. Each separation point is independently considered. The rate of vorticity shedding into the wake may be closely approximated by [13]

$$\frac{d\Gamma}{dt}=0.5U_s^2, \tag{3}$$

where U_s is velocity of the external flow at $\theta=\theta_s$ on the cylinder surface in the absence of the new vortex influence. This the strength of the nth point vortex is given by

$$\Gamma_n=0.5U_s^2\Delta t, \tag{4}$$

where Δt is the time increment. The new vortices are introduced into the flow at points

$$z_n=(1+\delta)\exp(i\theta_s), \tag{5}$$

where

$$\delta=\frac{2}{\frac{2\pi|U_s|}{|\Gamma_n|}-1} \tag{6}$$

is the dimensionless radial distance from the cylinder at $\theta=\theta_s$ determined by the requirement of zero tangential velocity component at point $z=\exp(i\theta_s)$ on the cylinder surface [12]. It is required that the no-slip condition is exactly satisfied only at the instant of each new vortex introduction. The images are simultaneously created to satisfy the condition of zero normal velocity at the surface. The generated vortices are convected with the local flow velocity at z_n at the time of their introduction.

4. Convection

The vortices are convected with the local velocity at their current position, e. g. under the action of the uniform flow past the cylinder and the velocity field generated by all other vortices. The induced velocity of each vortex, is determined by local complex velocity potential, which is being excluded (individual vortices do not contribute to their own velocity) which yields

$$u_n(t_k)+iv_n(t_k)=\frac{dz_n}{dt}\Big|_{t=t_k}=\frac{dW_n}{dz}\Big|_{z=z_n}, \tag{7}$$

where u_n and v_n are Cartesian velocity components of the nth convected vortex at time t_k. The new position of the nth vortex is specified from the difference scheme

$$z_n(t_{k+1})=z_n(t_k)+[u_n(t_k)+iv_n(t_k)]\,\Delta t \tag{8}$$

with Δt being the time step and $t_{k+1}=t_k+\Delta t$.

5. Lift and drag

Within the framework of an inviscid model the forces acting on the cylinder can be directly determined using the Lagally theorem. Lift and drag coefficients are computed from the positions, velocities, and strengths of the vortices and their images following the formula

$$C_D+iC_L=\sum_{n=1}^{N}\Gamma_n(iu_n-v_n)-\sum_{n=1}^{N}\Gamma_n(iu_{ni}-v_{ni}) \tag{9}$$

derived by Sarpkaya [14]. The suffix i in Eq. (9) denotes the image vortex. The velocities of real and image vortices are interrelated by

$$u_{ni}-iu_{ni}=\frac{-u_n+iv_n}{\bar{z}_n^2}. \tag{10}$$

6. Inducement of asymmetry

The symmetric vortex structure is unstable at high Reynolds numbers and asymmetry develops soon after an impulsive start which promotes the alternate vortex shedding [15, 16]. In numerical simulation of an impulsively started symmetrical flow, with no vorticity in the wake at the beginning, the flow pattern develops symmetrically. Thus, it is necessary to introduce disturbances of limited strength and duration into the flow in order to induce the shedding of the first vortex and the formation of an asymmetric vortex wake. In order to perturb the flow field the same sign point vortices in the wake are subjected to a small translation

$$z_n(t_{k+1})=z_n(t_k)+[u_n(t_k)+iv_n(t_k)]\,\Delta t+\Delta x \tag{11}$$

of the magnitude

$$\Delta x=0.04\left[1-\cos\left(\pi\frac{t_k-5}{4}\right)\right]\quad\text{for } 5<t_k<9 \tag{12}$$

gradually increasing with time [17].

7. Wake

The wake is modelled by a set of point vortices superimposed onto the potential flow about a cylinder. Under the assumption of an inviscid flow, the point vortex moves with the velocity determined by the local flow field and its strength remains constant in time. In real fluid the vortices which too closely approach the cylinder will be dissipated by the action of viscosity. In the absence of viscosity and the no-slip condition, imposed on the cylinder boundary, the individual vortices can approach

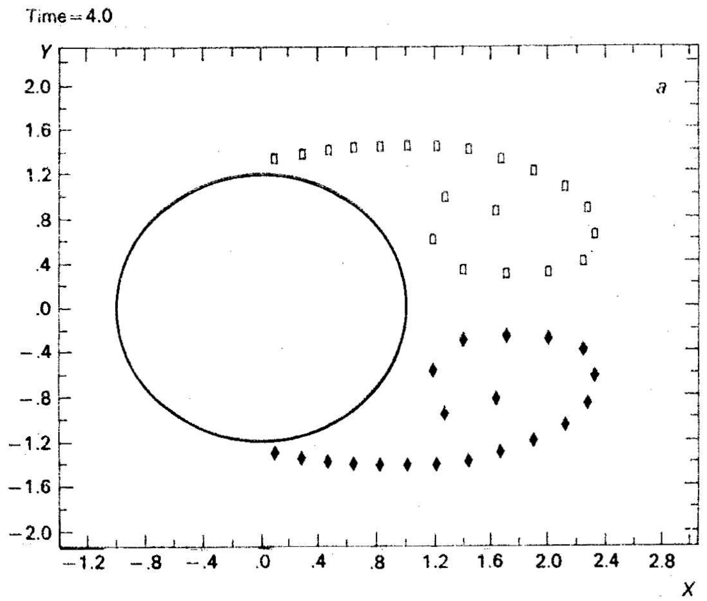
Time = 4.0
Y
2.0
1.6
1.2
.8
.4
.0
−.4
−.8
−1.2
−1.6
−2.0
a
−1.2
−.8
−.4
.0
.4
.8
1.2
1.6
2.0
2.4
2.8
X

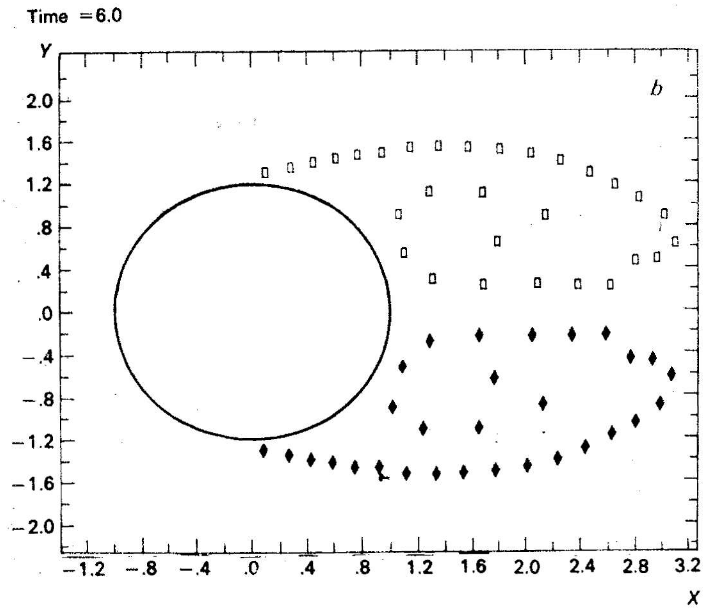
Time = 6.0
Y
2.0
1.6
1.2
.8
.4
.0
−.4
−.8
−1.2
−1.6
−2.0
b
−1.2
−.8
−.4
.0
.4
.8
1.2
1.6
2.0
2.4
2.8
3.2
X

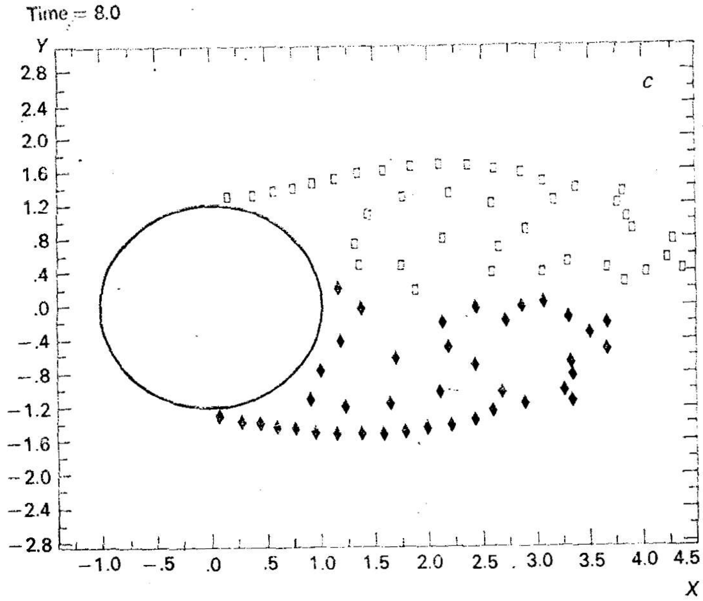
Time = 8.0
Y
c
2.8
2.4
2.0
1.6
1.2
.8
.4
.0
−.4
−.8
−1.2
−1.6
−2.0
−2.4
−2.8
−1.0 −.5 .0 .5 1.0 1.5 2.0 2.5 3.0 3.5 4.0 4.5
X

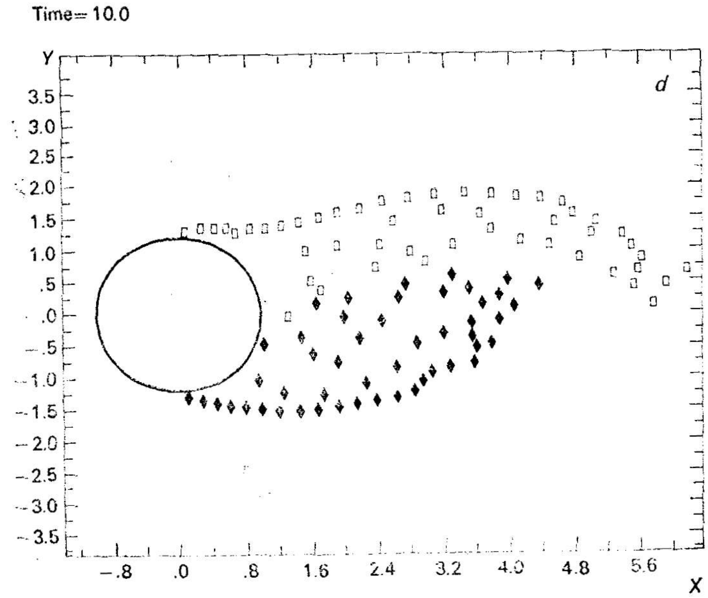
Time = 10.0
Y
d
3.5
3.0
2.5
2.0
1.5
1.0
.5
.0
−.5
−1.0
−1.5
−2.0
−2.5
−3.0
−3.5
−.8 .0 .8 1.6 2.4 3.2 4.0 4.8 5.6
X

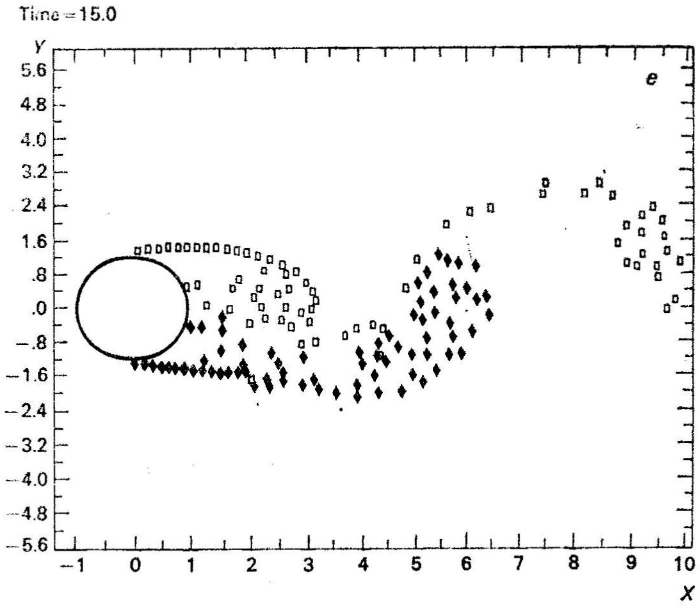
Time = 15.0
Y
5.6
4.8
4.0
3.2
2.4
1.6
.8
.0
−.8
−1.6
−2.4
−3.2
−4.0
−4.8
−5.6
e
−1
0
1
2
3
4
5
6
7
8
9
10
X

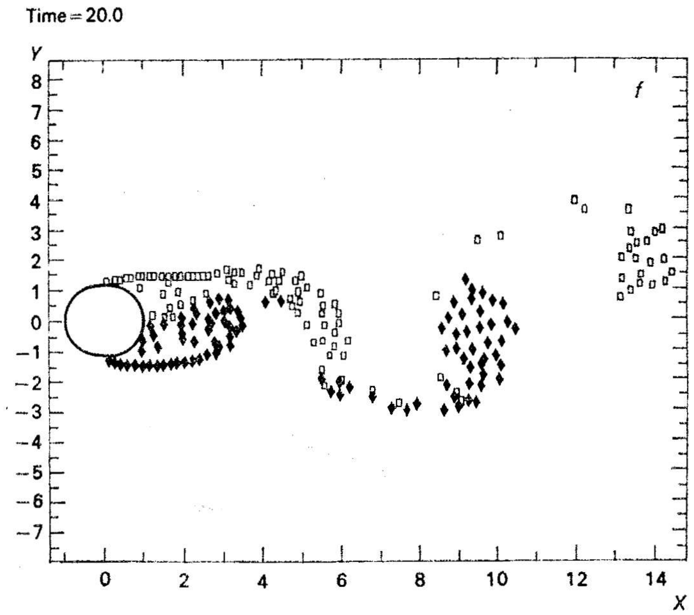
Time = 20.0
Y
8
7
6
5
4
3
2
1
0
−1
−2
−3
−4
−5
−6
−7
f
0
2
4
6
8
10
12
14
X

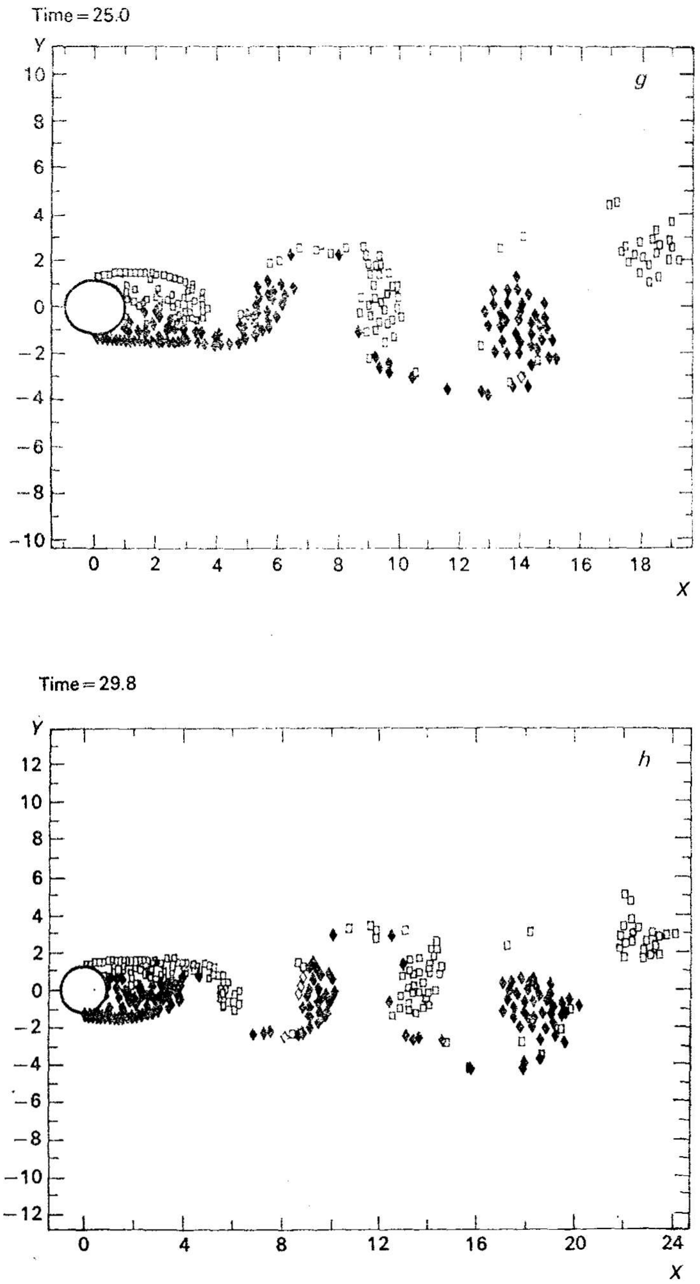

Fig. 2. a, b — positions of vortex centres at successive stages of wake development. □ and ■ denote point vortices with clockwise rotation and counter clockwise rotation, respectively; *c—h* — positions of vortex centres at successive stages of wake development; □ and ■ denote point vortices with clockwise rotation and counter clockwise rotation, respectively

one another or the cylinder surface (the images) very closely. However, in the neighbourhood of the point vortices, the fluid velocity tends to infinity.

Therefore, such vortices can acquire extremely high velocities. To avoid unreally high velocities in numerical simulation, the point vortices are eliminated from the flow field and calculation whenever they cross the cylinder or come closer to its surface than the radial distance of 0.04 [17], and they coalesce after having approached one another too closely. The following coalescence scheme is applied [18]: for $x<3$ the vortices coalesce if they come closer than 0.05, and for $x>3$ — if they come closer than 0.1 of the cylinder radius.

Most of the computation time is used for calculation of velocities. The computer time required to calculate the velocities of vortices increases almost proportionally to the square of the number of vortices [9]. In order to reduce the computer time for modelling the fully developed flow, the number of point vortices is minimized by coalesced ones which yields an equivalent velocity field (e. g. some vortices are replaced by a single point vortex of equivalent strength and situated at their gravity centre [5, 12]). The strength and position of the resulting vortex are given by

$$\Gamma=\sum_n \Gamma_n, \quad x=\frac{\sum_n |\Gamma_n| x_n}{\sum_n |\Gamma_n|}, \quad y=\frac{\sum_n |\Gamma_n| y_n}{\sum_n |\Gamma_n|}. \tag{13}$$

Besides, those vortices which drifted too far away from the cylinder are combined into a single vortex.

8. Discussion of numerical results

Some flow characteristics calculated for the angle of separation $\theta_s=80^0$ and time increment $\Delta t=0.2$ and 0.3 (time interval between the introduction of vortices) are shown in figures. Fig. 2*a*—*h* show the distribution of all point vortices at various time. The evolution of the two-dimensional wake is followed over a long time period after the start point. The newly introduced vorties leave the cylinder in two streams which interact and begin to form two symmetric coherent vortex stuctures behind the cylinder. Then the subsequent asymmetry develops and the vortex structures are alternately shed from either side of the cylinder. Finally, a configuration of point vortices develops, forming a rotational wake of alternate vorticity distribution. The average dimensionless spacing of the vortices in the completely developed region of the wake has been found equal 9.6 in the longitudinal direction and 2.9 in the transversal one. The lift and drag coefficients and the rate of vorticity shedding from two separations are plotted in Figs 3-5 as functions of time. The drag coefficient slightly fluctuates about the mean value of $C_D=1.3$. The lift coefficient oscillates with the mean amplitude of about 0.55 and oscillation frequency of 0.094. The fluctuations of $d\Gamma/dt$ and $C_L(t)$ for $t>5$ roughly have the same dominant frequency, which can be expressed by means of the Strouhal number, of about $S\approx0.19$. Figs 4 and 5 show that $|d\Gamma/dt|$ for the upper surface approximately is in phase with $C_L(t)$. After the initial transition, up to about $t=5$, these curves reflect clearly the periodic formation of vortices, and a comparison with Fig. 2 shows their correlation with the flow development. The mean drag coefficient and the Stouhal number of the vortex shedding (determined from the frequency of lift fluctuations or the fluctuations in the rate of vorticity shedding) are in a reasonable agreement with the experiment [8, 19]. The lift coefficient is rather

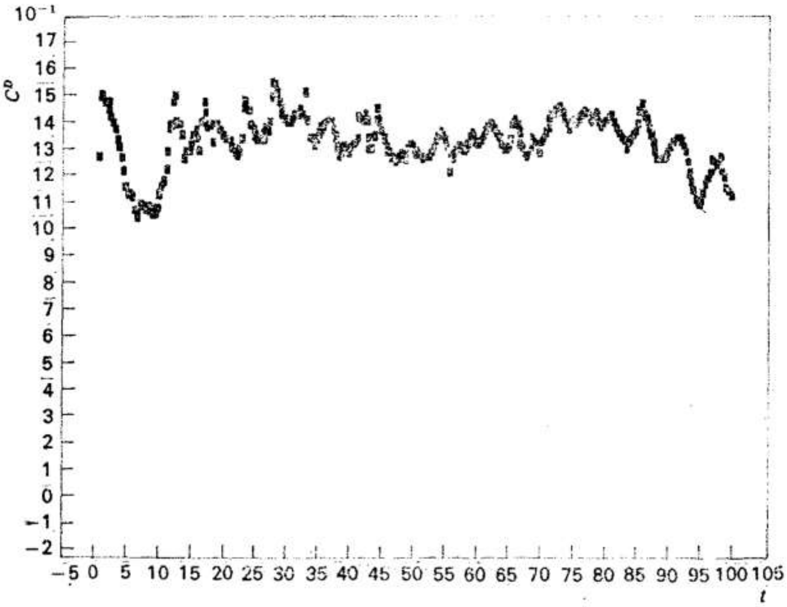

Fig. 3. Variation of drag coefficient versus time

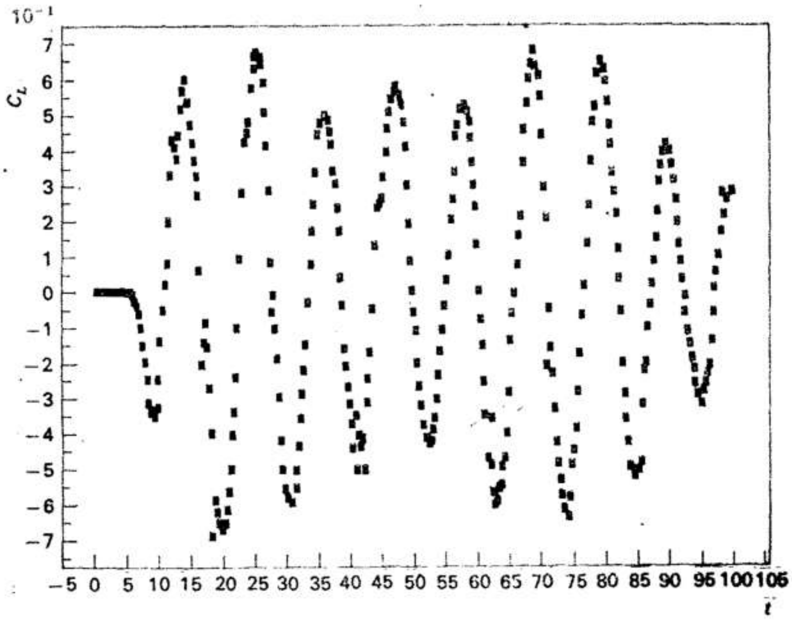

Fig. 4. Variation of lift coefficient versus time

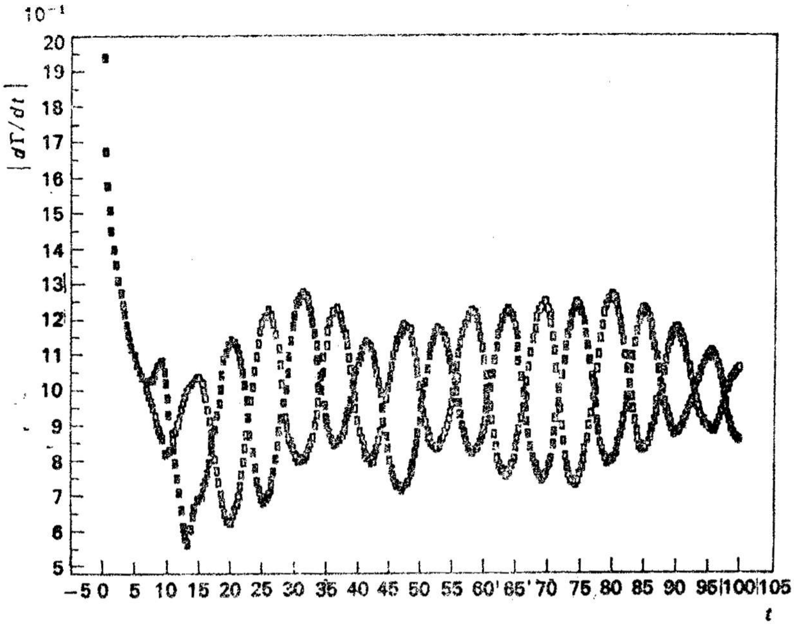

Fig. 5. Variation of the rate of shedding of positive ■ and negative □ vorticity versus time

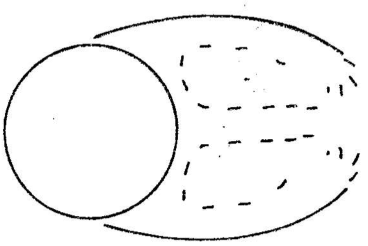

Fig. 6. Plot of the induced velocity of each point vortex in the flow of time t=6.0 and 25.0. The length of segments is proportional to the velocity of the corresponding vortices; their orientation indicates direction of movement

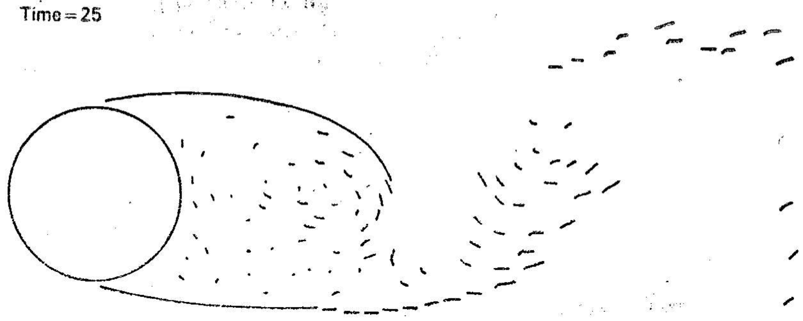

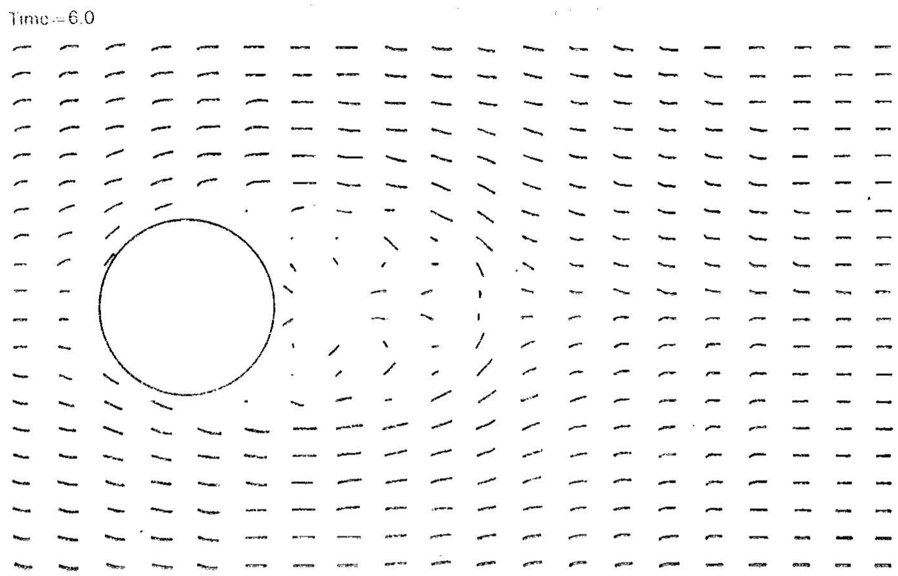

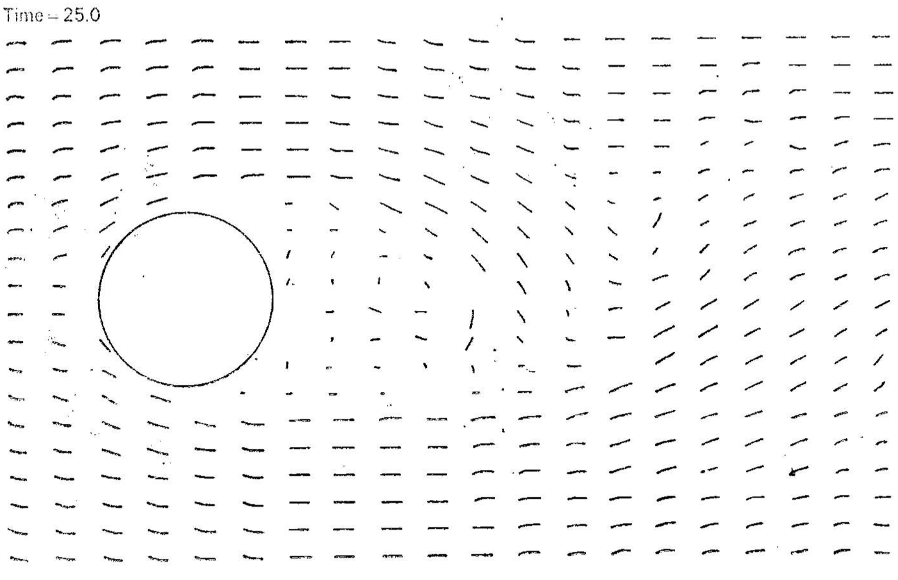

Fig. 7. Velocity vector field behind a circular cylinder at various time of the flow development. The length of segments is proportional to the local speed of fluid at their origin : their orientation indicates direction of the flow

overestimated. However, it is generally difficult to estimate it properly because of a large scatter of experimental results [19]. Plots of the velocity induced at each point vortex in the flow at time point $t=6.0$ and 25.0 are shown in Fig. 6. The length of the sections in the figures corresponds to the magnitude of the vortex velocity and the orientation indicates the direction of the movement. Fig. 7 consists of computer graphs of velocity vector field behind the circular cylinder at various time in the flow development. The length of the sections in the figures corresponds to the speed of the fluid at that point, and the orientation indicates the direction of the flow. The velocity vector fields shown in Fig. 7 correspond to the situation shown in Figs: *2b*, *2g*, and 6, respeĉtively.

9. Comments

Potential flow theory modelling and application of fhe discrete vortex method gives the main characteristics of the flow past a circular cylinder at high Reynolds numbers. Some results are in agreement with the experiments. A reasonable simulation of the real flow has been achieved assuming fixed separation points. The inviscid model simulates the physical situation in terms of vorticity. Therefore, the main influence on the vortex formation is exerted by vorticity itself.

References

1. Rosenhead, L. Formation of vortices from surface of discontinuity, — Proc. of the Royal Soc. of London., **134**, 1931, Ser. A, 170-192.
2. Sarpkaya, T. Computational methods with vortices. The 1988 Freeman School Lecture. — J. Fluids Eng. Trans ASME, **111**, 1988 No 1, 5-52.
3. Белоцерковский, С. М., В. Н. Котовский, М. И. Ништ, Р. М. Федоров. Математическое моделирование плоскопараллельного нестационарного отрывного обтекания тел. Москва, Наука, 1988.
4. Gerrard, J. H. Numerical computation of magnitude and frequency of the lift on a circular cylinder. — Philos. Transact. of the Royal Soc. of London, **261**. 1967, Ser. A, 137-162.
5. Laird, A. D. K. Eddy formation behind circular cylinders. — J. Hydr. Div. Proc. ASCE., **97**, 1971, HY 6, 763-775.
6. Mei, V. C., I. G. Currie. Flow separation on a vibrating circular cylinder. — The Phys. of Fluids, **12**, 1969, No 11, 2248-2254.
7. Toebs, G. H. The unsteady flow and wake near an oscillating cylinder. — J. of Basic Eng. Trans. ASME, **91**. 1969, No 4, 493-502.
8. Chen, Y. N. Fluctuating lift forces of the Karman vortex streets on single circular cylinders and the tube bundles. Part 1. The vortex street geometry of the single circular cylinder. — J. Eng. Ind. Trans. ASME. **94**, 1972, No 2, Ser. B, 603-610.
9. Chaplin, J. R. Computer model of vortex shedding from a cylinder. — J. Hydr. Div., Proc. ASCE, **99**, 1973, HY 1, 155-165.
10. Вальес, Н. Г. Расчет срывного обтекания цилиндра при автоколебаниях в потоке идеальной жидкости. - Изв. АН СССР. Механика жидкости и газа, 1980, № 3, 173-178.
11. Stansby, P. K. An inviscid model of vortex shedding from a circular cylinder in steady and oscillatory far flows. — Proc. Inst. Civil Eng., **63**, 1977, Part 2, 865-880.
12. Deffenbaugh, E, D. F. J. Marshal. Time development of the flow about an impulsively started cylinder. — AIAA J., **14**, 1976, No 7, 908-913.
13. Fage, A., F. C. Johansen. The structure of the vortex sheet. — Philos. Mag., 7, 1928, 417-436.

14. Sarpkaya, T. Lift, drag and added-mass coefficients for 30'‾ 1963, y derimmersed in a time-dependent flow. — J. Appl. Mech. Trans. ASME, ation of tN ol, Ser. E, 13-15.
15. Asher, J. A., D. S. Dosanj· An experimental investiget. — J.he formation and flow characteristics of an impulsively generated vortex stre of Basic Eng. Trans. ASME, 90, 1968, No 4, Ser. D., 596-606.
16. Nagata, H., Y. Kahei, M. Tsunekawa, T. Hasegawa. Unsteady flow past a circular cylinder started impulsively. — Bull. of the JSME, 18, 1975, 123, 992-1001.
17. Sarpkaya, T., R. L. Shoaff. Inviscid model of two-dimensional vortex shedding by a circular cylinder. — AIAA J., 17, 1979, No 11, 1193-1200.
18. Lewis, R. I., K. C. Shim. Vortex cloud analysis of the average and fluctuating flow past a cylinder in a uniform stream. — Sci. Papers of the Inst. of Mech. Construction and Operation of the Techn. Univ. of Wrocław. Conferences 9, 46, 1986, 145-161.
19. Попов, С. Г. О зависимости между числами Струхалия и Рейнольдса при плоском обтекании кругового цилиндра. — Изв. АН СССР. Мех. жидкости и газа, 1966, № 2, 156-159.

Received an May 31, 1990